Energy Proceedings
Vol 30, 2023
ISSN 2004-2965

Effect of inclination angle on the laminar flow of CO_2-mango bark nanofluid in inclined tube-in-tube heat exchanger

Uwadoka O[1], Adelaja AO[1,2*], Olakoyejo OT[1], Fadipe OL[3], Efe S[4**]

1 Department of Mechanical Engineering, University of Lagos, Akoka, Yaba, Lagos State, 101017, Nigeria

2 Visiting Professor, Faculty of Engineering and the Built Environment, Durban University of Technology, P.O. Box 1334, Durban, 4000, South Africa

3 Department of Industrial and Systems Engineering, Morgan State University, 1700 East Cold Spring Lane, Baltimore, Maryland

4 Department of Civil Engineering, Morgan State University, 1700 East Cold Spring Lane, Baltimore, Maryland

* Corresponding Author: aadelaja@unilag.edu.ng

** Alternative Corresponding Author: Steve.efe@morgan.edu

ABSTRACT

With over 50% of the world's population dwelling in urban areas, responsible for 75% of global energy consumption and 70% of greenhouse gas emissions, there is a need to ensure that urban energy systems are sustainable. One way to achieve this is to develop efficient energy systems that utilize captured and stored CO_2 as the working fluid. Also, the awareness of climate change and the environmental impact of human activities has necessitated research into using natural refrigerants and environmentally friendly nanoparticles in the heating, ventilation, and air conditioning (HVAC), process, chemical, nuclear, and energy sectors. Metallic and non-metallic nanoparticles have been studied extensively in the past few decades. Though they have improved the rate of heat energy transfer, the environmental impact assessment is questionable. The environmental impact of the common nanofluids necessitates the investigation of renewable bio-nanoparticles such as mango bark. The present study investigates the thermal and hydraulic characteristics of CO_2-mango bark nanofluids for application in gas cooling. The Reynolds number of the nanofluid is varied between 100 and 1000; nanoparticle volume concentration is between 0.5 and 2.0%, and the inclination angle is -90° to +90°. The heat transfer coefficient and pressure difference show a significant relationship with the inclination angle, Reynolds number and nanoparticle volume concentration. However, the heat transfer enhancement due to the nanofluid is about 10%, and the inclination angle is up to 40%. The inclination angle of ±30°, ±45°, and ±60° consistently possess higher thermal and hydraulic characteristics.

Keywords: Heat transfer enhancement, CO_2-mango bark nanofluid, gas cooling, convective heat transfer, inclined heat exchanger

NOMENCLATURE

Symbols	
ρ	density
k	thermal conductivity
C_p	specific heat at constant pressure
T	temperature
μ	viscosity
q	heat flux
h	heat transfer coefficient
Nu	Nusselt number
$\vec{v}$	velocity vector
Subscripts	
b	bulk
f	base fluid
in	inlet
nf	nanofluid
out	outlet
p	particle

1. INTRODUCTION

Increased rural-urban migration rates and population expansion, especially in the low-income sub-Sahara Africa and Southeast Asia, can enormously pressure basic infrastructure. On the global scale, urban energy systems account for about 75% of global energy consumption and 70% of greenhouse gas (GHG) emissions [1]. Therefore, the urban energy systems need to be sustainable given the climate sustainable development goals. The most significant of these goals is climate neutrality, i.e., the mitigation of the GHGs. To achieve this, it is to do away with fossil fuels, refrigerants with high global warming potentials (GWP) and ozone-depleting potentials (ODP), capture, store and utilize CO_2, develop efficient engineering systems, etc.

The re-visitation of CO_2 as a refrigerant was addressed by Lorentzen and Pettersen in 1992 [2] to tackle the above-mentioned environmental issues. However, a study by Brown et al. [3] confirmed that CO_2 performs worse than conventional refrigerants such as R22 in vapour compression systems. The transcritical CO_2 cycle was introduced, but it has also been associated with low energy performance due to expansion losses, according to Groll and Robinson [4].

The first mention of nanofluids in open literature was by Choi and Eastman [5]. Since then, numerous papers have been written on the performative characteristics of nanofluids in heat transfer applications. Leong et al. [6] reported that for a given air with Re = 6000 and coolant (Re = 5000), the use of copper nanoparticles helped to save 18.7% of frontal air area. Aktas et al. [7] found that when R600a/Al_2O_3 nanorefrigerant was utilized instead of R600a base refrigerant, there was a 43.93% increase in COP. Henderson et al. [8] examined the influence of SiO_2 nanoparticles with a volume fraction of 0.02 - 0.08 percent on the boiling thermal performance of HFC-134a and R-134a/ polyolester in a two-phase flow. When nanoparticles were mixed with HFC-134a refrigerant via direct dispersion, the heat transfer coefficient (HTC) was reduced by 55% compared to pure HFC-134a refrigerant. Conventional nanoparticle materials are harmful to humans and the environment, and therefore, human and environmentally benign bio-nanofluids are needed.

On the study of bio-nanofluid characteristics, Ajayi et al. [9] carried out energy consumption analyses of R290/Melon peel nanofluid as a replacement for HFC-22 refrigerant in air conditioning systems. The nanoparticles were dispersed in the base fluid at different concentrations. The nanofluid was found to perform better than HFC-22 in terms of energy consumption by using 15.2% less energy. Yadav and Singhai [10] reported that Al_2O_3 nanoparticles gave a higher Nusselt number and HTC, up to 5% than water-based mango bark nanofluids. Chen et al. [11] also reported that mango/water and palm kernel/water-EG nanofluids have lower thermal conductivity than conventional nanofluids. Furthermore, conventional hybrid nanofluids were noted to have the most significant thermal conductivity even with nanoparticle concentrations as low as 0.1%.

From the literature, it can be inferred that very limited research has been done on using CO_2-mango bark nanofluid to improve the thermal performance of a heat exchange system. To the best of the authors' knowledge, studies on the influence of inclination angle on the CO_2-mango bark nanofluid are rare in the literature. Therefore, this study aims to fill this gap using a numerical simulation approach (ANSYS-Fluent software).

2. MATERIALS AND METHODS

2.1 Model representation

CO_2-mango bark nanofluid flows through a pipe with an inner diameter d = 4.5 mm and length L = 970 mm at an initial temperature of 320K. The pipe wall is subjected to a heat flux q''= -10W/m^2, as shown in Fig. 1. The flow is incompressible and laminar with Re = 100 - 1000. The inclination angles (β) are ±90^o, ±60^o, ±45^o, ±30^o, and 0^o, and volume concentrations (φ) are 0, 0.5%, 1.0%, and 2.0%.

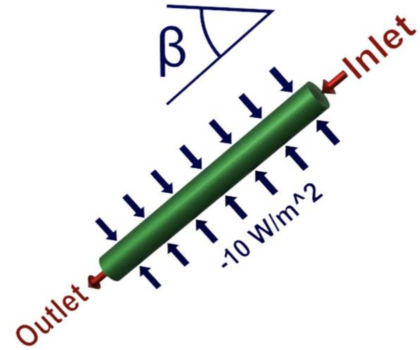

Fig. 1 Model representation

2.2 Governing differential equations

The current study assumes a 3D one-phase, steady-state flow with the thermal properties of the fluid kept constant. The conservations equations are given as:

$$\nabla.\vec{v} = 0 \quad (1)$$

$$\rho_f(\vec{v}.\nabla\vec{v}) = -\nabla p + \rho_f\vec{g}cos\beta + \mu_f\nabla^2\vec{v} \quad (2)$$

$$\left(\rho C_p\right)_f(\vec{v}\nabla T) = k_f\nabla^2 T \quad (3)$$

The energy transfer equation in the pipe is:

$$k_s\nabla^2 T = 0 \quad (4)$$

Where for copper pipe, k_s = 398 Wm^{-1}K^{-1}.

The boundary condition for the fluid-solid interface is:

$$k_f\frac{\partial T}{\partial n} = k_s\frac{\partial T}{\partial n} \quad (5)$$

No-slip condition is assumed at the channel wall:

$$\vec{v} = 0 \quad (6)$$

The boundary conditions for the temperature at the inlet and pressure outlet are given as:

$$T = T_{in} \quad (7)$$

$$p_{out} = p_{amb} \quad (8)$$

The solid external surface boundary,

$$q = -10\ Wm^2 \quad (9)$$

2.3 Thermo-physical properties

Maxwell's relations are used to calculate the properties of the nanofluid:

$$\rho_{nf} = \varphi\, \rho_p + (1-\varphi)\rho_f \tag{10}$$

$$\mu_{nf} = \mu_f(1 + 2.8\,\varphi) \tag{11}$$

$$C_{p\,nf} = \frac{\varphi\, \rho_p\, C_{p\,p} + (1-\varphi)\rho_f\, C_{p\,f}}{\rho_{nf}} \tag{12}$$

$$k_{nf} = k_f\left(\frac{k_p + 2\,k_f - 2\,\varphi\,(k_f - k_p)}{k_p + 2\,k_f + \varphi\,(k_f - k_p)}\right) \tag{13}$$

Where: ρ_f, ρ_p, ρ_{nf} are the densities of the base fluid, nanoparticle, and nanofluid, respectively. φ is the volume concentration, μ_f , μ_{nf} are the dynamic viscosities of the base fluid and nanofluid, respectively. $C_{p\,f}, C_{pp}, C_{p\,nf}$ are the specific heat capacities of the base fluid, nanoparticle, and nanofluid, respectively. Similarly, k_f, k_p, k_{nf} are the thermal conductivities of the base fluid, nanoparticle and nanofluid, respectively.

2.4 HTC calculations

The observed thermodynamic properties are the HTC:

$$h = \frac{q''}{T_w - T_f} \tag{14}$$

where T_f, T_w, and q'' are the average bulk, wall temperatures and heat flux, respectively.

2.5 Pressure difference calculation

The difference between the channel's upstream (p_{in}) and downstream (p_{out}) pressures were used to compute the pressure difference through the pipe. The following is the relationship for the pressure difference:

$$\Delta p = p_{in} - p_{out} \tag{15}$$

3. VALIDATION OF MODEL

3.1 Error calculation

The mean absolute deviation (MAD), root mean square error (RMSE) and mean square error (MSE) given in Eq. (16-18) are used to compare numerical results with experimental.

$$MAD = \frac{1}{N}\sum_{i=1}^{N}\frac{|x_i - \hat{x}_i| * 100}{\hat{x}_i} \tag{16}$$

$$RMSE = \sqrt{\frac{1}{N}\sum_{i=1}^{N}(x_i - \hat{x}_i)^2} \tag{17}$$

$$MSE = \frac{1}{N}\sum_{i=1}^{N}(x_i - \hat{x}_i)^2 \tag{18}$$

Where N is the number of data, X_i, the experimental values from other investigations, and $\hat{X}_i$ is the numerical simulation.

3.2 Grid independence test

Finite volume meshes with different numbers of grids were computed to find the best mesh. The fluid used in the pipe for this experiment was pure water with Re = 1050. To verify the grid independence of the various mesh element sizes, the outlet temperature was measured, as indicated in Table 1. The test was continued until the $\left|\frac{T_i - T_{i-1}}{T_i}\right| \le 1\%$. Between mesh with serial numbers 5 and 6, there is a 0.79% difference. The mesh consistency used across all simulations conducted for this investigation is serial number 5. Additionally, it was found that adding additional meshes after serial number 6 caused the results not to converge.

Table 1 Grid independence test

S/N	Number of Meshes	Outlet Wall Temperature (K)	Percentage deviation (%)
1	19,499	314.61	---------
2	38,597	321.90	2.32
3	59,941	340.20	5.69
4	101,166	335.06	1.51
5	234,971	329.63	1.62
6	301,534	327.02	0.79

3.3 Validation

Before beginning the analysis utilizing the CO_2-mango bark nanofluid, the dependability and accuracy of the simulation code and setup were verified. Shah's [12] equation, Wen and Ding's [13] experimental studies on water heat transfer, Heris et al. [14] convective heat transfer studies on Cu/Water nanofluids, and Nourafkan et al. [15] convective heat transfer and pressure difference of Cu/Water nanofluid were used to validate the model.

The errors between the current and validated studies are displayed in Table 2. Shah's equation shows that the mean absolute deviation has a maximum value of 31.45%. The fact that Shah's equation was modeled for pipes with bigger diameters may be the source of the considerable deviation. For all other investigations, the mean absolute deviation is less than 20.0%. Figs. 2-4 show the graph plots comparing the results of this study and the validated studies.

4. RESULTS

4.1 Thermal performance

Plots of the HTC versus β for various volume fractions at Re = 100, 400, 700, and 100 are shown in Figs. 5-8. It can be seen that for all Re, there is a comparable relationship between HTC and β. The results show a clear increase in HTC with nanofluid volume concentration, primarily due to increased particle collision. Other researchers have also reported increases in the HTC of various nanofluids. For example, for mango bark water,

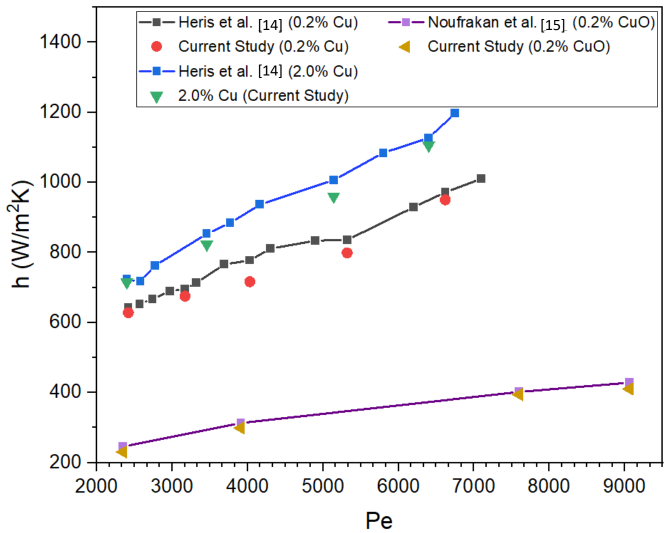

Fig. 2 Comparison of current study for HTC with experimental data of a) Heris et al [14], and b) Noufrakan et al [15]

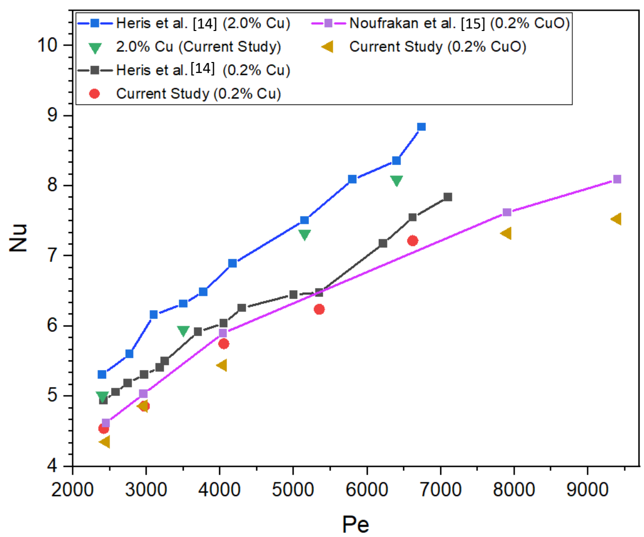

Fig. 3 Comparison of current study for Nusselt Number with experimental data of a) Heris et al [14], and b) Noufrakan et al [15]

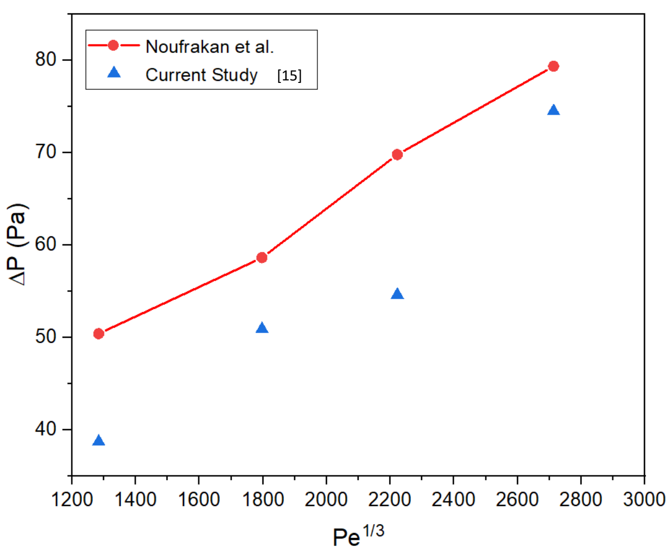

Fig. 4 Comparison of current study for pressure difference with the experimental data of Noufrakan et al [15]

Onyiruike et al. [16, 17], the hybrid of Alumina and Cu in water suspension [18, 19]. As expected, the 2.0% vol. fraction nanofluid exhibits the maximum HTC in most instances. For all values of Reynolds number except 100, the HTC rises with β from -90°. It peaks at -45°, falls to a low at 0°, and rises again at +45° before falling to another low at +90°. However, for Re = 100, the oscillatory trend still applies, but the peaks occur at -30° and +60°. The minimum values for the HTC mostly occur at ±90°. This variation might result from the thermal boundary layer being affected by gravitational force as the angle varies. The HTC also increases with respect to the Re. This relationship is due to the fact that since velocity is directly related to the Re, an increase in the latter allows for an increase in mass transfer and convection rate in the fluid. A peak β of +45° was also noted by Senthilkumar et al. [20] and Akbari et al. [21]. For very low mass fluxes, Uwadoka et al. [22] reported peak β of -45° and +60°.

4.2 Pressure difference

Plots of the pressure difference versus β for various volume concentrations at Re = 100, 400, 700, and 1000 are shown in Figs. 9-12. The plots show a clear relationship between the volume fraction and pressure difference in the nanofluid. As the volume fraction increases, the pressure difference increases in all cases, with the highest values of pressure difference occurring at 2% and the lowest at 0%. This phenomenon might be as a result of the increase in viscosity as the volume fraction increases. An increase in viscosity encourages a higher rate of friction losses in the flow. There also exists a relationship between Re and the pressure difference because as Re increases, an apparent increase is seen in the pressure difference as well. Lastly, it can be seen that for all Re values except 100, the pressure difference rises from -90°, increases through -60°, and peaks at -45°. Afterward, it drops back down through -30° to a low at 0°; it then rises to a new peak at +45° and descends to a low at +90°. For Re = 100, however, the pressure difference at -90° is almost equal to that of -60°.

Table 2 Statistical analysis of validated data

Studies	Plots	MSE	RMSE	MAD (%)
Shah [12]	H_2O: Nu vs x/D	2.75	1.66	31.45
Wen and Ding [13]	H_2O: Nu vs Re	3.41	1.85	13.99
	0.2% Cu/H_2O nanofluid: Nu vs Pe	0.12	0.35	6.31
	0.2%Cu/H_2O nanofluid: Nu vs Pe	0.08	0.29	5.18
Heris et al. [14]	0.2% Cu/H_2O nanofluid: h vs Pe	1440.5	37.95	4.11
	0.2% Cu/H_2O nanofluid: h vs Pe	896.6	29.94	2.89
	0.2% Cu/H_2O nanofluid: h vs. Pe	447.5	21.16	5.35
Nourafkan et al. [15]	0.2% Cu/H_2O nanofluid: Nu vs Pe	0.14	0.37	5.61
	ΔP vs $Pe^{1/3}$	112.88	10.62	19.95

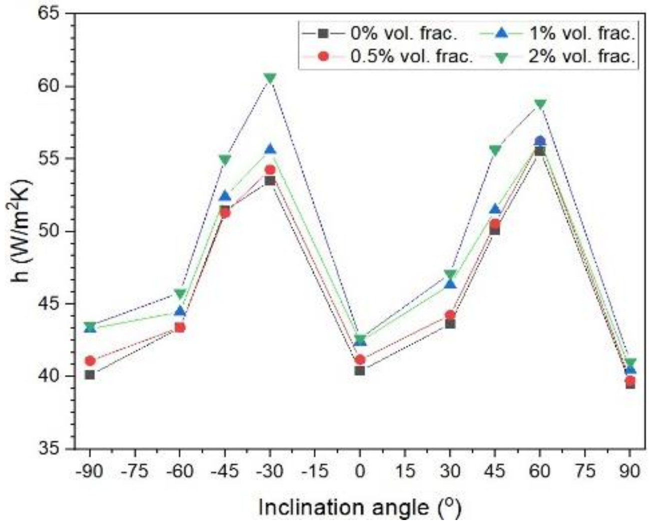

Fig. 5 HTC versus β for Re = 100

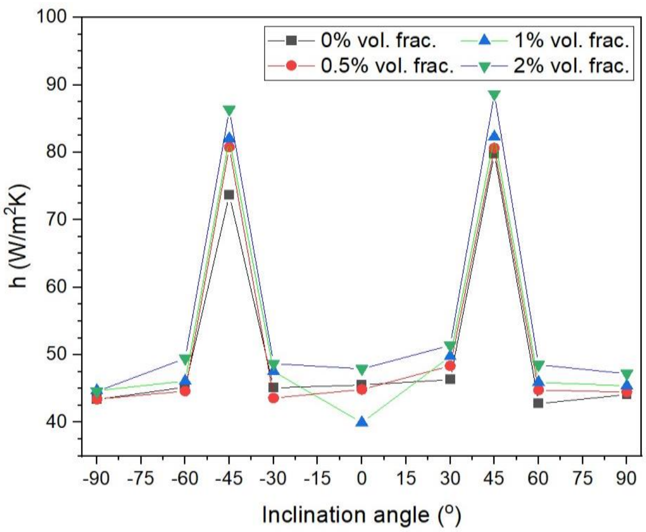

Fig. 6 HTC versus β for Re = 400

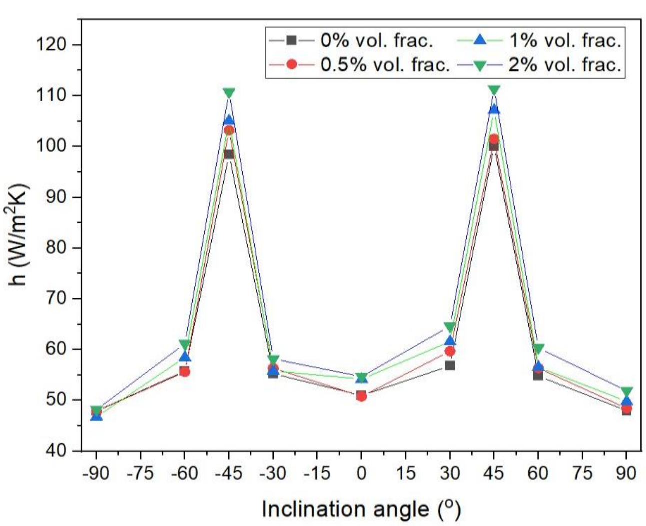

Fig. 7 HTC versus β for Re = 700

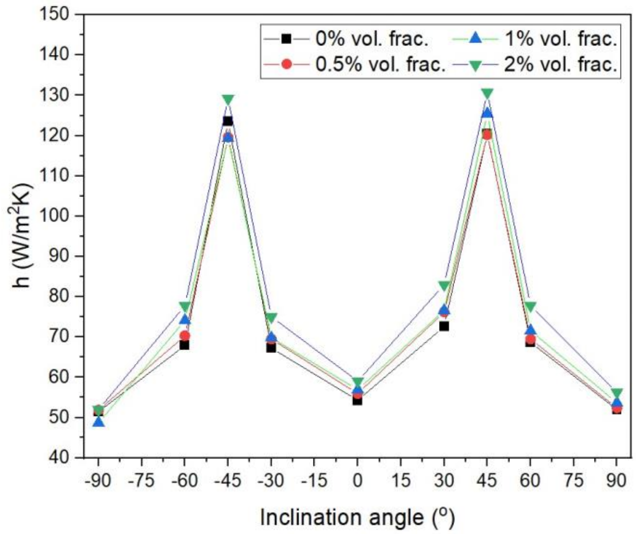

Fig. 8 HTC versus β for Re = 1000

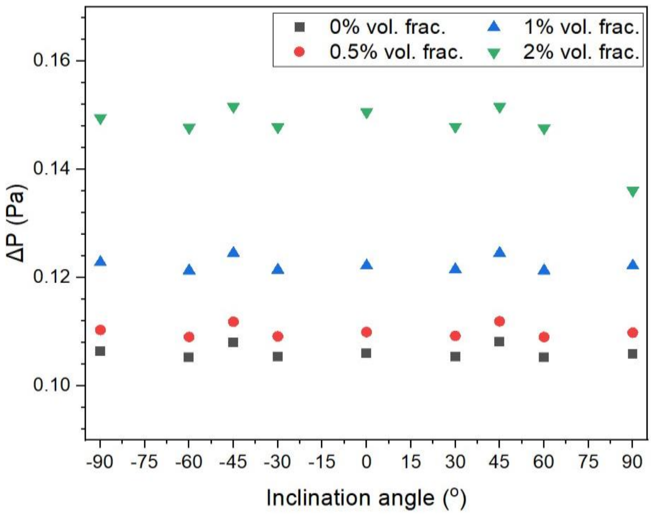

Fig. 9 Pressure difference versus β for Re = 100

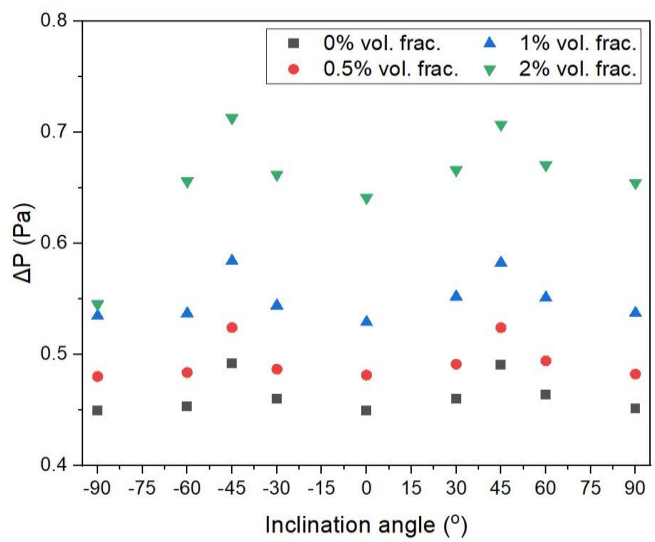

Fig. 10 Pressure difference versus β for Re = 400

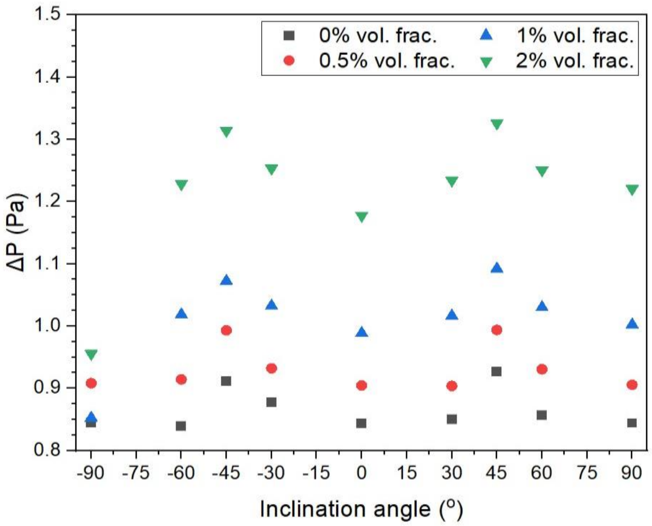

Fig. 11 Pressure difference versus β for Re = 700

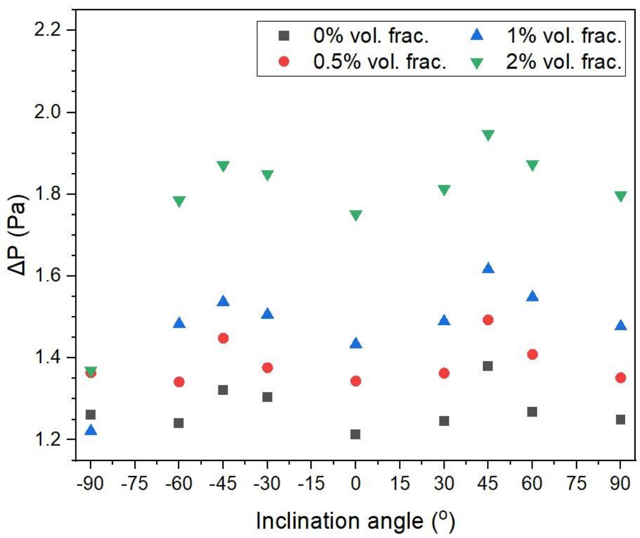

Fig. 12 Pressure difference versus β for Re = 1000

On the contrary, Uwadoka et al. [22] noted that β did not significantly influence the pressure gradient.

5. CONCLUSION

Mango Bark/CO_2 nanofluid heat transfer and hydraulic properties through a circular pipe are investigated. In order to do the numerical simulation, ANSYS Fluent was used. On the thermal and hydraulic properties, the impact of the inclination angle, nanofluid volume concentration, and Reynolds number are examined. The HTC and pressure difference are significantly affected by the Reynolds number, inclination angle, and volume concentration, such that an increase in the Reynolds number and volume concentration causes an increase in the heat transfer coefficient (HTC) and pressure difference. For the HTC and pressure difference, the peak inclination angles occur at ±45° for Re = 400 – 1000, whereas for Re = 100, the peaks occur at -30° and +60°.

ACKNOWLEDGEMENT

The authors appreciate the support from the University of Lagos, Akoka, Nigeria and Morgan State University, Maryland, USA, to present this paper at CUE2022.

REFERENCES

[1] Klemm C, Wiese F. Indicators for the optimization of sustainable energy urban systems based on energy system modeling. Energy Sustain and Soc 2022;12(3):1-20.

[2] Lorentzen G, Pettersen J. A new efficient and environmentally benign system for car air-conditioning. *Int J Refrig* 1993;*16*(1): 4-12.

[3] Brown J, Kim Y, & Domanski P. Evaluation of carbon dioxide as R-22 substitute for residential air-conditioning / Discussion. *ASHRAE Transactions* 2002; *108*.

[4] Groll DM, & Robinson EA. Efficiencies of transcritical CO2 cycles with and without an expansion turbine. *International Journal of Refrigeration* 1998; *21*(7): 577-589.

[5] Choi S, Eastman JA. Enhancing thermal conductivity of fluids with nanoparticles. United States,1995

[6] Leong K, Saidur R, Kazi S., Mamun A. Performance investigation of an automotive car radiator operated with nanofluid-based coolants (nanofluid as a coolant in a radiator). *Applied Thermal Engineering* 2010; *30*(17-18): 2685-2692.

[7] Aktas M, Dalkilic A, Celen A. A Theoretical Comparative Study on Nanorefrigerant Performance in a Single-Stage Vapor-Compression Refrigeration Cycle. *Advances in Mechanical Engineering* 2014; *7*(1).

[7] Henderson K, Park Y-G, Liu L, Jacobi AM. Flow-boiling heat transfer of R-134a-based nanofluids in a horizontal tube. *International Journal of Heat and Mass Transfer* 2010; *53*(5-6): 944-951.

[9] Ajayi OO, Okolo TI, Salawu EY, Owoeye FT, Akinlabu DK, Akinlabi ET, Akinlabi ST, Afolalu SA. Performance and energy consumption analyses of R290/Bio-based nanolubricant as a replacement for R22 refrigerant in air-conditioning system. Energy Technology 2019; 103-112.

[10] Yadav RK, Singhai A. Heat transfer enhancement in a double pipe heat exchanger using bio-nano fluid (mango-bark) using CFD. International Journal of Innovative Research in Technology 2020; 6(9): 123-130.

[11] Chen J, Oumer A, Azizuddin A. A review on thermo-physical properties of bio, non-bio and hybrid nanofluids. *Journal of Mechanical Engineering and Sciences* 2019; *13*(4).

[12] Shah R. Thermal entry length solutions for the circular tube and parallel plates. *Proceedings of 3rd National Heat and Mass Transfer Conference 1* 1975:11-75. Bombay: Indian Institute of Technology

[13] Wen D, Ding Y. Experimental investigation into convective heat transfer of nanofluids at the entrance region under laminar flow conditions. Int J Heat Mass

Transf 2004; *47*(24):5181–5188
[14] Heris S, Etemad SG, Esfahany MN. Convective Heat Transfer of a Cu/Water Nanofluid Flowing Through a Circular Tube. *Exp Heat Transf* 2009; *22*(4): 217-227.
[15] Nourafkan E, Karimi G, Moradgholi J. Experimental Study of Laminar Convective Heat Transfer and Pressure difference of Cuprous Oxide/Water Nanofluid Inside a Circular Tube. *Exp Heat Transf* 2015; *28*(1): 58-68.
[16] Onyiriuka EJ, Ighodaro OO, Adelaja AO, Ewim DRE, Bhattacharyya S A numerical investigation of the heat transfer characteristics of water-based mango bark nanofluid flowing in a double-pipe heat exchanger. Heliyon 2019;5: e02416.
[17] Onyiriuka EJ, Obanor AI, Mahdavi M, Ewim DRE. Evaluation of single-phase, discrete, mixture and combined model of discrete and mixture phases in predicting nanofluid heat transfer characteristics for laminar and turbulent flow regimes, Adv.Powder Technol. 2018; 29 (11) 2644–2657.
[18] Omosehin, OS, Adelaja, AO, Olakoyejo, OT. Numerical study of the thermal performance and pressure differences of water-based Al_2O_3 - Cu hybrid nanoluids of different compositions in a microchannel heat sink. Microfluid Nanofluidics 2022a; 26 (49).
[19] Omosehin OS, Adelaja AO, Olakoyejo OT, Oluwatusin OO, Oyekeye OM, Abolarin SM. Numerical Study of the Thermal-Hydraulic Performance of Water-Based Al_2O_3 - Cu Hybrid Nanofluids in a Double-Layer Microchannel Heat Sink. Energy Proceedings 2022b;1-5.
[20] Senthilkumar R, Vaidyanathan S, Sivaraman B. Effect of inclination angle in heat pipe performance using copper nanofluid. Procedia Eng. 2012;38, 3715-3721.
[21] Akbari M, Behzadmehr A, Shahraki F. Fully developed mixed convection in horizontal and inclined tubes with uniform heat flux using nanofluid. Int. J. Heat Fluid Flow 2008; 29(2):545-56.
[22] Uwadoka O, Adelaja AO, Noah OO, Fadipe OL, Lee SW. Numerical Investigation of Heat Transfer and Pressure difference Characteristics of CO_2-mango bark Nanofluid in inclined Gas Cooling Process. Energy Proceedings 2022;1-5.